Carbohydrate Polymers 116 (2015) 149–158

Contents lists available at ScienceDirect

Carbohydrate Polymers

journal homepage: www.elsevier.com/locate/carbpol

Antifouling coating of cellulose acetate thin films with polysaccharide multilayers

Tamilselvan Mohan[a,*,1], Rupert Kargl[b], Karin Eva Tradt[a], Martin R. Kulterer[a], Matej Bračić[b], Silvo Hribernik[b], Karin Stana-Kleinschek[b,2], Volker Ribitsch[a,2]

[a] Institute of Chemistry, Karl-Franzens-University Graz, Heinrichstraße 28, 8010 Graz, Austria
[b] Institute for the Engineering and Design of Materials, University of Maribor, Smetanova 17, 2000 Maribor, Slovenia

ARTICLE INFO

Article history:
Received 11 November 2013
Received in revised form 11 April 2014
Accepted 15 April 2014
Available online 26 April 2014

Keywords:
Cellulose acetate thin films
Chitosan
Carboxymethyl cellulose
Quartz crystal microbalance
LbL method
BSA adsorption

ABSTRACT

In this investigation, partially deacetylated cellulose acetate (DCA) thin films were prepared and modified with hydrophilic polysaccharides with the layer-by-layer (LbL) technique. As polysaccharides, chitosan (CHI) and carboxymethyl cellulose (CMC) were used. DCA thin films were manufactured by exposing spin coated cellulose acetate to potassium hydroxide solutions for various times. The deacetylation process was monitored by attenuated total reflectance-infrared spectroscopy, film thickness and static water contact angle measurements. A maximum of three bilayers was created from the alternating deposition of CHI and CMC on the DCA films under two different conditions namely constant ionic strengths and varying pH values of the CMC solutions. Precoatings of CMC at pH 2 were used as a base layer. The sequential deposition of CMC and CHI was investigated with a quartz crystal microbalance with dissipation, film thickness, static water contact angle and atomic force microscopy (AFM) measurements. The versatility and applicability of the developed functional coatings was shown by removing the multilayers by rinsing with mixtures containing HCl/NaCl. The developed LbL coatings are used for studying the fouling behavior of bovine serum albumin (BSA).

1. Introduction

Besides other materials, cellulose acetate (CA) was one of the first polymers used for filtration membranes in water purification (Kutowy & Sourirajan, 1975). CA is a renewable and bio-based material which exhibits several reliable properties such as moderate hydrophilicity, high biocompatibility, good desalting properties, and a high potential flux (Han, Zhang, Shao, Kong, & Lv, 2013; Hayama, Yamamoto, Kohori, & Sakai, 2004). Despites its advantages, CA has poor fouling resistance, which is caused by the accumulation of biological foulants (bacteria, cells, proteins, *etc.*,) on the membrane surface (Jones & O'Melia, 2001; Koseoglu-Imer, Dizge, & Koyuncu, 2012). Fouling can lead to a drastic decline in permeate flux, filtration efficiency and lifetime of a membrane. To overcome this, surface functionalization of the CA substrate is an option. Among other techniques, available the layer-by-layer (LBL) technique is a simple and straightforward approach. This method is based on the alternate exposure of a substrate to positively and negatively charged components. It provides the possibility to introduce a large variety of functional materials into a coating (Findenig et al., 2012; Hadj Lajimi, Ferjani, Roudesli, & Deratani, 2011). This makes the technique a powerful tool to create customized antifouling surfaces. Polysaccharides (PS) are promising materials for creating such surfaces due to their diverse chemical composition (Bauer et al., 2013). Even though multilayer coatings from water soluble PS are known, (Hadj Lajimi et al., 2011; Radeva, Kamburova, & Petkanchin, 2006) their influence on the protein rejection behavior has not been studied extensively. Hadj Lajimi et al. (2011) investigated the LbL assembly of chitosan and alginic acid on CA membranes. The BSA coated surfaces were subsequently tested for their salt rejection properties (Hadj Lajimi et al., 2011). Keeping this fact in mind, we became interested if chitosan (CHI) and carboxymethyl cellulose (CMC) on CA can be used for reducing the fouling of BSA (Jeyachandran, Mielczarski, Rai, & Mielczarski, 2009).

Both, chitosan and CMC are renewable, biocompatible, nontoxic and biodegradable (Bulwan al., 2012). CMC is negatively charged in aqueous solution and can adsorb irreversibly on cellulose-based substrates (*e.g.* deacetylated cellulose acetate) *via*

* Corresponding authors at: University Graz, Institute of Chemistry, Heinrichstraße 28/3, 8010 Graz, Austria. Tel.: +43 163805413.
E-mail addresses: tamilselvan.mohan@uni-graz.at (T. Mohan), rupert.kargl@um.si (R. Kargl).
[1] Tel.: +43 316 380 5413.
[2] Member of the European Polysaccharide Network of Excellence (EPNOE).

http://dx.doi.org/10.1016/j.carbpol.2014.04.068
0144-8617/

relatively selective cellulose-cellulose interactions (Kargl et al., 2012; Laine, Lindstrom, Nordmark, & Risinger, 2002). CHI, a positively charged PS, has found application in the medical field (*e.g.* drug delivery), and is also able to bind CMC irreversibly *via* complex formation (Zhang, Chen, Li, & Liu, 2007; Zhang et al., 2013).

To obtain a better understanding and control on the growth of the multilayers under different pH (Schoeler, Poptoshev, & Caruso, 2003; Shiratori & Rubner, 2000) and charge densities, (Glinel, Moussa, Jonas, & Laschewsky, 2002; Schoeler, Kumaraswamy, & Caruso, 2001) it is advantageous to use thin CA model films (*ca.* 30 nm thickness) instead of membranes. Membranes exhibit great complexities in terms of composition, roughness, morphology, which often leads to results that are not directly comparable. However, model films consist of thin coatings on flat substrates and can be manufactured by a simple spin coating technique. In this case, a comprehensive characterization of the substrates can be carried out and modern surface analytical techniques can be utilized. One such technique for monitoring *in situ* self-assembly of charged PS on thin films is the quartz crystal microbalance with dissipation (QCM-D) (Dixon, 2008; Findenig, Kargl, Stana-Kleinschek, & Ribitsch, 2013). QCM-D allows studies on the interaction of dissolved polymers or proteins with thin solid films by measuring the frequency changes of an oscillating quartz crystal. Furthermore, QCM-D allows to probe polymer–polymer interaction, complex formation, surface hydration and viscoelastic properties of the adsorbates. The purpose of this study was therefore to prepare deacetylated cellulose acetate (DCA) model films, to explore their properties and to use them for the deposition of multilayers from CMC and CHI. To elaborate and develop the built up of thin LbL films from these polyelectrolytes two different methods were employed. In the first method, the same ionic strength and pH value was used for both polyelectrolyte solutions. In the second method, the pH value was varied for electrolyte free CMC solutions and kept constant for the CHI solutions. The potential application of the developed coatings is shown in the fouling behavior of BSA.

2. Experimental

2.1. Material and methods

Cellulose acetate (CA, acetyl content: 39.8 wt.%, degree of substitution, DS: 2.5, molecular weight, M_w: 30 kDa), sodium salt of carboxymethyl cellulose, (CMC, DS: 0.7, M_w: 90 kDa), chitosan, CHI (deacetylation: 75–85%, low molecular weight, viscosity at 25° (1 wt.%, in 1 wt.% acetic acid) 20–300 mPa s, product Number: 448869), bovine serum albumin (fraction V, ≥96%), disodium phosphate heptahydrate ($Na_2HPO_4{\cdot}7H_2O$), sodium dihydrogen phosphate monohydrate ($NaH_2PO_4{\cdot}H_2O$) and glacial acetic acid (≥99.7%) were purchased from Sigma-Aldrich, Austria. 1,4-dioxane was purchased from Carl Roth GmbH, Austria. Silicon wafers with a thickness of 100 nm and a surface orientation of 100 was purchased from Silchem, Freiburg, Germany. Surfs (SiO_2) substrates were purchased from Nanolane, France. QCM-D sensors coated with a gold layer (QSX301) were purchased from LOT-Oriel, Germany. Double distilled water was used for all sample preparations.

2.2. Substrate cleaning and thin film preparation

For spin coating of cellulose acetate, three different substrates were used. Silicon wafers were cut into pieces of $2 \times 2\ cm^2$, rinsed with ethanol (Sigma-Aldrich, Austria), rinsed with pure water and immersed into a "piranha" solution (H_2SO_4 (98 wt.%)/H_2O_2 (30 wt.%), 70:30, v/v) for 15 min. Afterwards the wafers were rinsed with water, stored in water for at least 15 min and blow-dried with nitrogen gas. QCM-D-sensors were soaked into a mixture of H_2O/H_2O_2 (30 wt.%)/NH_4OH (5:1:1; v/v/v) for 10 min at 70 °C, then immersed in a "piranha" solution for 40 s, and then rinsed with pure water and blow dried with nitrogen gas. Surfs (SiO_2) were used as received. Cellulose acetate was dissolved in 1,4-dioxane ($10\ g\ l^{-1}$), stirred for 2 h at room temperature, filtered using a 0.2 μm PTFE filter. 100 μl of the cellulose acetate solution were deposited onto a cleaned substrate and then rotated for 60 s at a spinning speed of 4000 rpm and an acceleration of 2500 rpm s^{-1}. All spin coated substrates were dried at 50 °C in an oven for 12 h, cooled to room temperature and eventually stored for further use.

2.2.1. Deacetylation of cellulose acetate (CA) films

Spin coated CA films were placed into polystyrene petri-dishes (4 cm in diameter). 15 ml of 0.1 M potassium hydroxide solution was deposited in the petri-dish. The films were immersed in the KOH solution for different times (0, 10, 20, 25, 30, 40, 60 min). The films were soaked into pure water (15 ml) for 10 min twice and finally blow dried with nitrogen gas.

2.3. Sample preparation for multilayer coatings and protein adsorption

The concentration of chitosan was 0.1% (w/v). The pH of the solution was adjusted to pH 3 with glacial acetic acid until complete dissolution and then to 5.5 with 0.1 M NaOH (Sigma-Aldrich, Austria). The carboxymethyl cellulose concentration (for LbL method I) was 0.1% (w/v) at pH 5.5. The pH of the solution was adjusted using 0.1 M HCl. In both cases, the ionic strength of the solutions was adjusted to 150 mM with potassium chloride (KCl). Carboxymethyl cellulose, 0.2% (w/v) (for pre-coating of DCA) at pH 2 and 0.1% (w/v) (for LbL method II) at pH 2, 3, 4 and 5.5 were prepared by adjusting the pH with 0.1 M HCl with no additional electrolyte. BSA ($10\ mg\ ml^{-1}$) was dissolved in 10 mM phosphate buffer (PBS) at pH 7. The ionic strength of the buffer solution was adjusted to 100 mM with NaCl.

2.4. Attenuated total reflectance-infrared (ATR-IR) measurements

ATR-IR spectra were recorded for spin coated CA and DCA films using a PerkinElmer Spectrum GX Series-73565 FTIR-spectrometer at a scan range of 4000 to 650 cm^{-1}. A total of 32 scans were performed for all measurements with a resolution of 4 cm^{-1}. QCM-D Au-sensors were used as substrates.

2.5. Quartz crystal microbalance with dissipation (QCM-D)

A QCM-D device (model E4 from Q-Sense, Gothenburg, Sweden) was used to investigate the multilayer coatings from CMC and CHI on the DCA films. The QCM-D instrument determines changes in frequency (f) and dissipation (D) of an oscillating quartz crystal. Deposition of mass or changes in the rigidity of material on the crystal surface can be detected. Negative frequency shifts (Δf) indicate a deposition of mass whereas positive dissipation shifts (ΔD) are caused by a reduced rigidity of the coating. The QCM-D measurements were conducted at the fundamental frequency of 5 MHz and its overtones. A detailed description of the QCM-D technique can be found elsewhere (Höök, Rodahl, Brzezinski, & Kasemo, 1998; Rodahl, Höök, Krozer, Brzezinski, & Kasemo, 1995). For the data analysis in this study, the changes in the third overtone's frequency and dissipation (Δf_3, ΔD_3) were used. For all QCM-D experiments, sensors coated with DCA films were mounted into the QCM-D flow cell and the initial resonance frequency of the sensor was measured. Afterwards, the films were equilibrated with pure water followed by rinsing with the background solution (pH 2 water or 150 mM KCl at pH 5.5) until a constant frequency was established. Two types

of multilayer coatings were performed in the QCM-D, denoted as method I and II.

In method I, DCA films were incubated with CMC (0.2%; w/v) at pH 2 (no additional electrolyte) for 15 min and rinsed with pure water for 10 min. Following this, the CMC coated surfaces were alternatingly coated with solutions of CHI (0.1%; w/v) at pH 5.5/150 mM KCl, and CMC (0.1%; w/v) at pH 5.5/150 mM KCl for 15 min. Between each coating step, the substrates were rinsed with water for 10 min. In sum three CMC/CHI bilayers were deposited onto CMC pre-coated DCA films. As a comparison, multilayer coatings were created onto DCA films without a pre-coating of CMC at pH 2.

In method II, DCA films were pre-coated with CMC (0.2%; w/v) at pH 2 for 15 min (no additional electrolyte) followed by rinsing with water for 10 min. Afterwards, the CMC coated DCA films were coated alternatively with CHI (0.1%; w/v) at pH 5.5/150 mM KCl and with CMC at pH 2, 3, 4 and 5.5 respectively without additional electrolyte for 15 min. After each coating step, the layers were rinsed with pure water for 10 min. Three bilayers of CMC/CHI were constructed. The flow rate was kept at 0.1 ml min^{-1} throughout all experiments. All measurements were performed at $21 \pm 0.1\,^{\circ}C$.

2.5.1. Stability test

The stability of the three bilayer coatings obtained from method II was additionally tested. The coatings were rinsed with solutions containing 5 M NaCl and 50 mM HCl for 15 min followed by pure water for 10 min.

2.5.2. Protein adsorption

The three bilayers constructed from CMC at pH 2, 3 and 5.5 according to method II were used for protein adsorption. Before protein injection, the multilayers were rinsed with PBS buffer (pH 7) until a stable frequency was obtained (60 min). After this, BSA (10 mg ml^{-1}) dissolved in PBS buffer was introduced into the cell for 30 min followed by BSA-free PBS buffer (30 min).

All measurements were carried using three independently coated sensors and an average value was calculated.

2.6. Sarfus-film thickness determination

For film thickness determination, LbL coatings were performed (on DCA films that were coated on surf substrates) by dip coating method. The same coating sequences (method I and method II) as described in the QCM-D measurement were used. For the dip coating the CMC coated or uncoated DCA films were dipped into the corresponding polyelectrolyte (CHI or CMC), electrolyte solution and water. All solutions were stirred constantly during coating and rinsing. After finishing the coating, the substrates were blow dried with nitrogen gas and stored at ambient conditions. Three independently coated sensors were used for each LbL coating.

The film thickness of uncoated and coated DCA films was determined using the Sarfus-technique. All measurements were obtained using a LEICA DM4000 optical microscope with Sarfusoft software (Nanolane, France). Surfs substrates ($1 \times 1\,cm^2$) coated with DCA films were used for the multilayer built-up. Each sample was probed on at least three spots with a 20 fold magnification. Three independent samples were used for each type of film and an average value was calculated. The absolute thickness of each film was determined *via* calibration with a step-height standard. A detailed explanation on the Sarfus-technique can be found elsewhere (Ausserré & Valignat, 2006).

2.7. Static water contact angle (SCA(H_2O)) measurements

For SCA(H_2O) determination, LbL coatings were performed (on DCA films that were coated on silicon wafers $2 \times 2\,cm^2$) by dip coating method as described in Section 2.6.

SCA of water were measured by using Dataphysics contact angle measurement system OCA15+ (Dataphysics, Germany) with the sessile drop method and a drop volume of 3 μl. All measurements were carried out at room temperature on uncoated and coated DCA films. Determination of the SCA was based on the analysis of the drop shape and was performed with the software provided by the manufacturer (software version SCA 20). All the measurements were performed on at least three independent substrates with a minimum of three drops per surface and an average value was calculated.

2.8. Atomic force microscopy (AFM)

The surface morphology of the films was characterized by atomic force microscopy (AFM) in tapping mode with an Agilent 5500 AFM multimode scanning probe microscope (Digital Instruments, Santa Barbara, CA). The images were scanned using silicon cantilevers (ATEC-NC-20, Nanosensors, Germany) with a resonance frequency of 210–490 kHz and a force constant of 12–110 N m^{-1}. All measurements were performed at room temperature.

3. Result and discussion

3.1. Cellulose acetate (CA) film characterization: Structure, thickness and wettability

The ATR-IR spectra of spin coated cellulose acetate (CA) films before and after deacetylation are shown in Fig. 1a. CA films, show characteristic peaks for —C═O, —C—O and —C—CH_3 at 1749, 1251 and 1376 cm^{-1} (Kim, Nishiyama, & Kuga, 2002). In the case of deacetylated cellulose acetate (DCA) films (10 to 30 min), the emergence of hydroxyl groups (as indicated by a broad peak at ~3244 cm^{-1}) and the subsequent reduction of the C = O peak are observed (Kargl et al., 2012). This proves that CA films are partially converted into DCA by treatment with KOH. After 30 min, peaks that correspond to acetyl groups are vanished and the intensity of the hydroxyl groups is increased.

Besides that, the appearance of structural features in the region 950–1200 cm^{-1} is changed and a new pattern that corresponds to cellulose is detected. This confirms that between 40 and 60 min of treatment, the CA films are converted into cellulose films (Kontturi, Thüne, & Niemantsverdriet, 2003; Mohan et al., 2011). With this approach we could show that it is possible to tailor CA films with a tunable hydrophilic and cellulose character.

Fig. 1b shows the comparison of Sarfus-film thickness and static water contact angles for CA films that were deacetylated for different times. Untreated CA films show a film thickness of 71 ± 0.4 nm and a CA(H_2O) of $61 \pm 0.2^{\circ}$, similar to the values obtained in our previous work (Kargl et al., 2012). As expected film thickness and CA(H_2O) decrease with increasing deacetylation. A relatively constant film thickness (29 nm) and wettability (CA(H_2O): 19°) are obtained after 40 min (Mohan et al., 2011; Mohan et al., 2012).

3.2. LBL coating from CHI and CMC at pH 5.5 (method I)

3.2.1. QCM-D studies

The QCM-D curves from the LbL coatings manufactured at pH 5.5 in 150 mM KCl are presented in Fig. 2. Since our aim was to employ CA films having partially hydrophilic/hydrophobic character for creating antifouling coatings with hydrophilic polysaccharide multilayers, CA films that were deacetylated for 25 min were used as

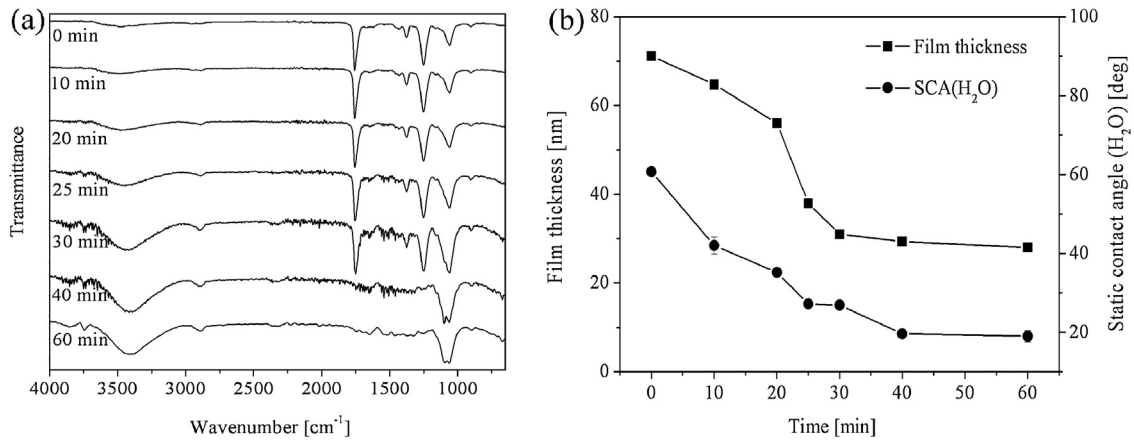

Fig. 1. (a) ATR-IR spectra and (b) comparison of film thickness and static water contact angle of cellulose acetate coated on gold substrates after different times of deacetylation with 0.1 M KOH.

substrates. The DCA films were pre-coated in the QCM-D chamber with CMC (0.2%; w/v) at pH 2. As a comparison, non-pre-coated DCA films were used. Fig. 2 shows the frequency and dissipation shifts (3rd overtone) for three bilayers. The deposition of CMC at pH 2 and subsequent rinsing with water, leads to a frequency shift of -55.7 ± 0.9 Hz. Rinsing with water did not show an increase in frequency but a positive shift in dissipation. This confirms that the CMC layer is irreversibly attached to the DCA film but strongly swells in pure water. Since the isoelectric point of carboxylic groups of CMC is 3.2, CMC is fully protonated and exhibits lower solubility at pH 2 (Fras et al., 2004; Hoogendam et al., 1998). Although no obvious precipitation occurred during the pH adjustment of the CMC solution, the solubility of CMC is lower at a pH below the p*K* value (3.8) (Fras et al., 2004). The irreversible deposition of CMC at pH 2 can be related to the specific interaction of unsubstituted glucose units of CMC with the DCA surface (having partially cellulose character), reduced charge and low solubility (Kargl et al., 2012).

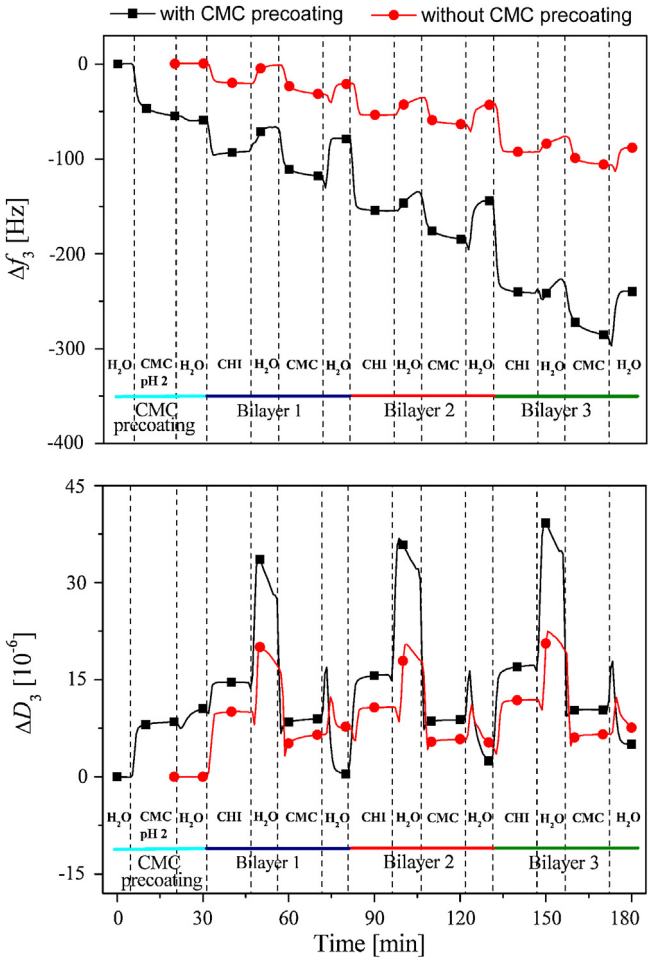

Fig. 2. Changes in frequency (upper figure) and dissipation shifts (lower figure) from the sequential deposition of CHI and CMC on DCA film, pre-coated with CMC at pH 2 (squares) and uncoated DCA film (circles). *Note*: CMC 0.2% at pH 2 (no electrolyte) was used for pre-coating. For LbL assembly, CMC (0.1%) and CHI (0.1%) solution prepared with 150 mM KCl at pH 5.5 were used.

For CMC pre-coated DCA films, a larger decrease in frequency was detected for the first CHI step showing that higher amounts of CHI are deposited when negative charges from CMC are present. After rinsing with water, loosely attached material is removed and a stable coating of CHI remains on both films but more CHI can be found on CMC pre-coated films after three bilayers. Chitosan is a weak polybase and positively charged at acidic conditions with a p*K*a of 6.0 (Čakara, Fras, Bračič, & Kleinschek, 2009). The presence of additional electrolyte will minimize the repelling forces along and between the charged CHI chains in solution, leading to change in conformation and reduced solubility (Findenig et al., 2013). Altogether, this will lead an enhanced deposition of CHI. After rinsing with pure water stable layers are formed through complexation of charges. The subsequent application of CMC (at pH 5.5) shows a strong interaction with the CHI layer. Upon rinsing with water, desorption of CMC is noted as indicated by an increase in frequency. This implies that, the solubility of CMC is increased as soon as it interacts with pure water, leading to desorption.

The final frequency shifts after three deposited bilayers are much larger on CMC pre-coated films even if the frequency shift from the pre-coating is considered (−240 Hz for the CMC pre-coated and −86 Hz for the uncoated DCA film). The CMC pre-coating serves as a negatively charged support for attaching significantly higher amounts of positively charged CHI. As a consequence more CHI is adsorbed, leading to a cumulating effect of enhanced deposition of both polyelectrolytes. Therefore a CMC pre-coating can be in general useful if one aims at immobilizing positively charged functional molecules onto usually uncharged DCA surfaces.

Dissipation gives information on the rigidity of the formed layers. Higher dissipation indicates softer and swollen layer whereas decreased dissipation is usually a result of a more rigid layer (Schlenoff, Rmaile, & Bucur, 2008; Schönhoff et al., 2007). An

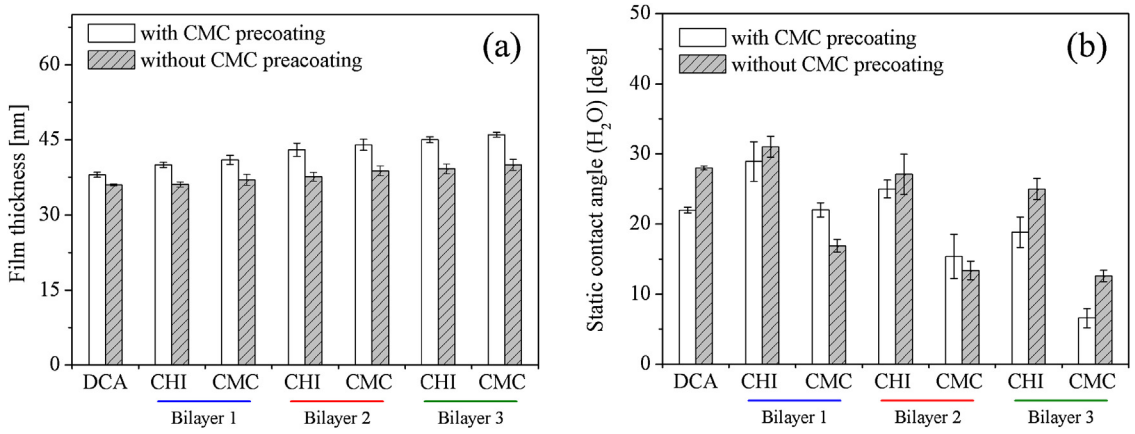

Fig. 3. (a) Film thickness and (b) static water contact angles and on surfaces obtained by the sequential deposition of CHI and CMC on CMC pre-coated and uncoated DCA films. *Note*: CMC 0.2% at pH 2 (no electrolyte) was used for pre-coating. For LBL assembly, CMC (0.1%) and CHI (0.1%) solutions in 150 mM KCl at pH 5.5 were used.

increased dissipation is visible after the first CHI immobilization on both uncoated and CMC pre-coated DCA films. These changes in dissipation are at the same level for each CHI deposition (Iturri Ramos, Stahl, Richter, & Moya, 2010; Lee, Ryu, & Youn, 2012). The replacement of the polyelectrolyte solution with pure water shows a strong increase in dissipation, revealing that a more extended and open structure is formed. In this case, the increase in dissipation can be explained by a strong swelling caused by the removal of ions and the incorporation of water. The change in dissipation is nearly the same for all CHI layers upon switching from the polyelectrolyte to pure water. Interestingly, the LbL film only strongly swells when the outermost layer is chitosan (Iturri Ramos et al., 2010). This is a result of more CHI than CMC being irreversibly deposited. Such a swollen layer can facilitate the interpenetration of further polyelectrolyte molecules (Liu, Zhao, Sun, & Zhang, 2008a; Liu, Zou, Fu, & Zhang, 2008b). In comparison, each CMC coated surface showed a strong decrease in dissipation which is constant for all CMC deposition steps. This can be attributed to the detachment of CMC and the formation of a more rigid structure through charge complexation between CHI and CMC. As a consequence, water molecules trapped inside the previous layers are expelled and a denser layer is formed. Simultaneously, a charge reversal takes place and the surface charge changes from positive to negative, allowing the subsequent adsorption of CHI (Liu et al., 2008a,b). Removal of water molecules also increases the frequency value. Upon switching to pure water, a sharp increase followed by a decrease in the dissipation is observed. This behavior can be related to changes in the density of the solution, dehydration and partial desorption of the outermost CMC layer.

3.2.2. Film thickness and surface wettability

The film thickness of multilayers from CHI and CMC at pH 5.5 in the presence of electrolyte is depicted in Fig. 3a. The DCA film coated with CMC (0.2%, w/v) at pH 2 showed a higher layer thickness (38 ± 0.3 nm) compared to uncoated films ($36\,\text{nm} \pm 0.1$). This proves in accordance with the QCM-D data that CMC is successfully deposited on the DCA film at a low pH. The dry film thickness of multilayer films for both, pre-coated and uncoated DCA films increases with the number of coating steps. For three bilayers, the maximum layer thickness on pre-coated DCA was *ca.* 46 ± 0.5 nm. However, the DCA film with no pre-coating showed only a layer thickness of 40 ± 0.4 nm. This emphasizes the role of CMC (at pH 2) as a base layer to immobilize more CHI and subsequently more CMC.

The sequential deposition of polysaccharides is expected to alter the wettability of the DCA surface. This is confirmed by the static water contact angle ($SCA(H_2O)$) of the coatings (Fig. 3b). The $CA(H_2O)$ on DCA films is decreased from $28 \pm 0.3^\circ$ to $22^\circ \pm 0.5$ after coating with CMC at pH 2. Differences in the wettability of the DCA film can be observed for each coated surfaces. In general, decreased wettability is observed when CHI forms the outermost layer. A higher wettability of CMC terminated surfaces confirms that the CMC layer is a more hydrophilic polymer than CHI which is also a result of the lower charge and insolubility of CHI at neutral pH. Yuan et al. (2007) also showed the lower wettability for CHI terminated surfaces when the multilayer film was constructed from chitosan and alginate. The effect of alternating wettability was even more pronounced for the CMC pre-coated films. This indicates that a higher surface coverage with more deposited material is achieved. In addition, other parameters such as thickness, surface topography, conformation of the adsorbed polymer and amount of incorporated ions can influence the wettability of the surface (Iturri Ramos et al., 2010; Kontturi, Tammelin, Johansson, & Stenius, 2008; Lee et al., 2012).

3.3. LBL coating from CHI and CMC at different pH values (method II)

3.3.1. QCM-D studies

In this section, the multilayer built-up from CHI at pH 5.5 in 150 mM KCl and CMC at different pH-values without additional electrolyte is presented. Since it was observed that a CMC precoating enhances the deposition of CHI, we have employed the same condition for the multilayer built up with method II. The QCM-D results that correspond to three multilayers are shown in Fig. 4. As can be seen much larger frequency shifts are detected at lower pH values owing to the lower solubility of CMC in the protonated form. At each pH value, higher frequency shifts are observed when CMC is deposited. When the layers are rinsed with pure water, loosely bound material is removed as reflected in increasing frequency values. Three bilayers built-up with CMC at pH 2 show the highest frequency shift ($\Delta f_3 = -1163.7 \pm 5.3$ Hz). Since CMC is a weak polyelectrolyte, its charge density increases with increasing pH (Hoogendam et al., 1998; Kästner, Hoffmann, Dönges, & Hilbig, 1997). At pH 2, far below the p*K*a value of carboxylic groups, CMC is uncharged, adopts a coiled structure and has a low solubility in water (Fujimoto & Petri, 2000). As the pH increases, the intra- and interchain repulsion between the CMC molecules increases which promotes an extended conformation and a strong increase in solubility (Kästner et al., 1997). Since CMC is uncharged at pH 2, it is expected that there is no electrostatic interaction with fully charged CHI. However, QCM-D results show a high deposition of

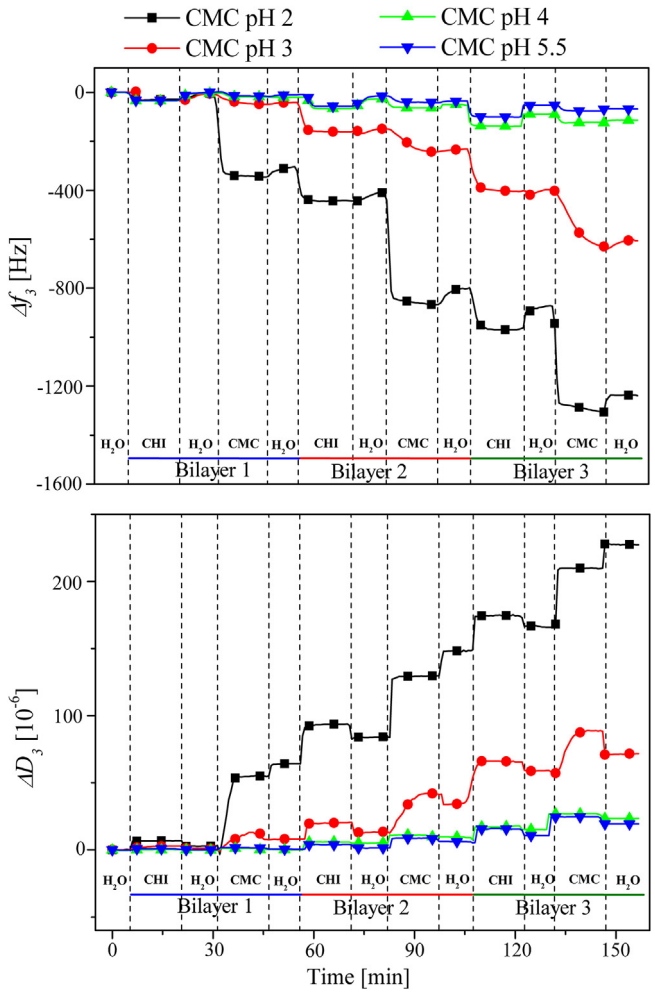

Fig. 4. Change in frequency (top) and dissipation (bottom) obtained from the sequential deposition of CHI and CMC at different pH values on DCA films pre-coated with CMC at pH 2. *Note*: CMC 0.2% at pH 2 (no electrolyte) was used for pre-coating. For LbL assembly a CHI (0.1%) solution in 150 mM KCl at pH 5.5 and CMC (0.1%) at pH 2–5.5 without the addition of electrolyte were used.

CMC onto CHI for each bilayer. As mentioned before, reduced solubility, charge and the formation of larger aggregates are the main driving forces for higher depositions rates. At pH 3, CMC is partially charged and more prone to an extended conformation (Fujimoto & Petri, 2000). Increased electrostatic repulsion of immobilized CMC and higher solubility prevents further deposition of the polyelectrolyte and lower amounts of material are deposited. This effect is more pronounced at higher pH values (4 and 5.5). The interaction of CHI with a charged CMC layer resulted in lower frequency shifts but higher amounts are deposited at low pH values when more CMC is present on the surface.

Contrary to coating method I, a constant and stepwise increase in dissipation after each polyelectrolyte deposition is observed mainly caused by the much higher amounts of irreversibly bound CMC. This data indicates a non-rigid hydrogel-like structure (Kontturi et al., 2008). During coating at pH 2, the dissipation always increases upon rinsing the CMC coated surfaces with water. These suggest that a rather strong swelling and reorganization of the CMC layer takes place. Upon contact with pure water, the CMC layer is deprotonated and swells. Electrostatically repelled CMC molecules are detached and a firmly attached but swollen CMC layer remains. This strong swelling causes the increased dissipation. In contrast a decrease in dissipation is observed when CHI coatings are rinsed with water, implying that the reversibly immobilized CHI polymer is removed and adopts a flat and extended conformation. Thus by simply tuning the pH of the CMC solution, the adsorption and conformation of CMC can be altered.

In addition, we investigated the same multilayer built-up (*i.e.* CMC at pH 2) on pure non-deacetylated CA films in order to examine the role of deacetylation and CMC interaction with CA surfaces and its consequences for the multilayer formation (see Fig. S2). QCM-D results showed that the adsorbed CMC layer is removed upon rinsing with water as indicated by the frequency value ($f_3 = -0.4 \pm 0.2$ Hz). This indicates that the interaction between CMC and pure CA surface is almost negligible. Subsequent introduction of CMC at pH 2 or CHI, confirmed that the deacetylation of CA and a subsequent pre-coating of CMC are beneficial for the LbL assembly.

3.3.2. Film thickness and surface wettability

The film thickness for three bilayers made from CHI and CMC at different pH values is shown in Fig. 5a. For all pH-values, the layer thickness increases with the number of coating steps. Multilayers made from CMC at pH 2 give a maximum film growth. These results are comparable with the QCM-D data (Fig. 4) where a maximum frequency shift was observed at the lowest pH value. An increase in layer thickness can also be seen for every CHI coating step, confirming that CHI significantly bound to the CMC coated surfaces. At pH 2 the film thickness increased by 7 nm with the first bilayer. After the second and the third bilayer, a thickness increase of 20 and 36 nm was observed. For the coatings performed at pH 3, 4, and 5.5, the maximum increase in layer thickness was 22, 13 and 4 nm after three bilayers respectively. As a result, the coating thickness can easily be adjusted by the pH value of the CMC solutions which is highly advantageous for functional multilayer coatings.

The wettability of multilayers created from alternating deposition of CHI at pH 5.5 and CMC at different pH values are shown in Fig. 5b. As expected, the water wettability of all CMC terminated surfaces increased significantly compared to uncoated DCA films. After three bilayers very hydrophilic materials are obtained. Similar to coating method I, CHI terminated surfaces show a decreased wettability leading to an alternating change in the static water contact angle. For the coatings manufactured with CMC at pH 2, a high water wettability is already reached after the first CHI-CMC bilayer, confirming the high deposition rates of CMC in the first step.

3.4. Stability and removal of the multilayer films

Further, we have investigated the stability of the three bilayers on DCA films manufactured according to method II. The coatings were rinsed with solution containing both high ionic strength and acid (5 M NaCl–50 mM HCl) followed by rinsing with pure water. This condition was chosen to verify a possible removal of the coatings for cleaning purposes of for instance coated membranes. The QCM-D data and thickness values before and after rinsing are shown in Fig. 6. A large reduction of frequency and an increase in dissipation can be observed after the introduction of the NaCl/HCl mixture into the QCM cell irrespective of the pH of CMC solution used for multilayer built-up (Fig. S1). This effect is caused by the density changes of the solutions. After rinsing with pure water, a strong increase in frequency and a decrease of film thickness is detected. This confirms that parts of the multilayer manufactured at pH 2 are dissolved and removed as a result of treatment with 5 M NaCl–50 mM HCl mixture. Multilayers that were manufactured at pH 3, 4 and 5.5 were almost completely removed. This demonstrates that, depending on the manufacturing conditions, one can control the stability and removability of the functional LbL coatings.

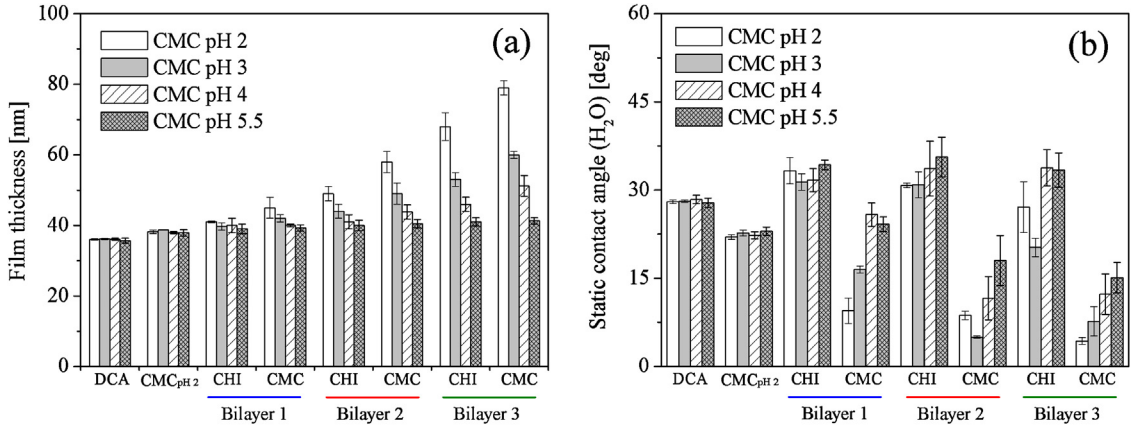

Fig. 5. Film thickness (a) and static water contact angles (b) on films obtained from the sequential deposition of CHI at pH 5.5/150 mM KCl and CMC at different pH values (2–5.5) coated on DCA after pre-coating with CMC at pH 2. *Note*: CMC 0.2% at pH 2 (no electrolyte) was used for pre-coating. For LbL assembly, CHI (0.1%) solutions were prepared with 150 mM KCl at pH 5.5 and CMC (0.1%) was prepared at pH 2–5.5 without the addition of electrolyte.

3.5. Surface topography

3.5.1. Coating method I

The surface morphology of multilayer coatings manufactured with method I is shown in Fig. 7(a–b). The morphology of the DCA film is changed after coating with three bilayers. A clear difference in the morphology is found for non-pre-coated films. Multilayers created onto CMC pre-coated films show a particle-like structure whereas multilayers formed without a CMC pre-coating show a fiber-like morphology. This effect is most likely caused by the particle like deposition of the CMC pre-coating (Kargl et al., 2012). These features (Fig. 7a–b) are retained even after the depositing of three bilayers.

3.5.2. Coating method II

Interesting surface features were obtained for three bilayer coatings from CHI at pH 5.5 and CMC at different pH values (Fig. 7c–f). Multilayer coatings from CMC at pH 2 clearly show the formation of large agglomerates and high RMS values. This confirms that high amounts of polyelectrolytes are deposited owing to the strongly reduced solubility of CMC. At pH 3 (Fig. 7d), smaller particles are observed and the root mean square roughness decreases as

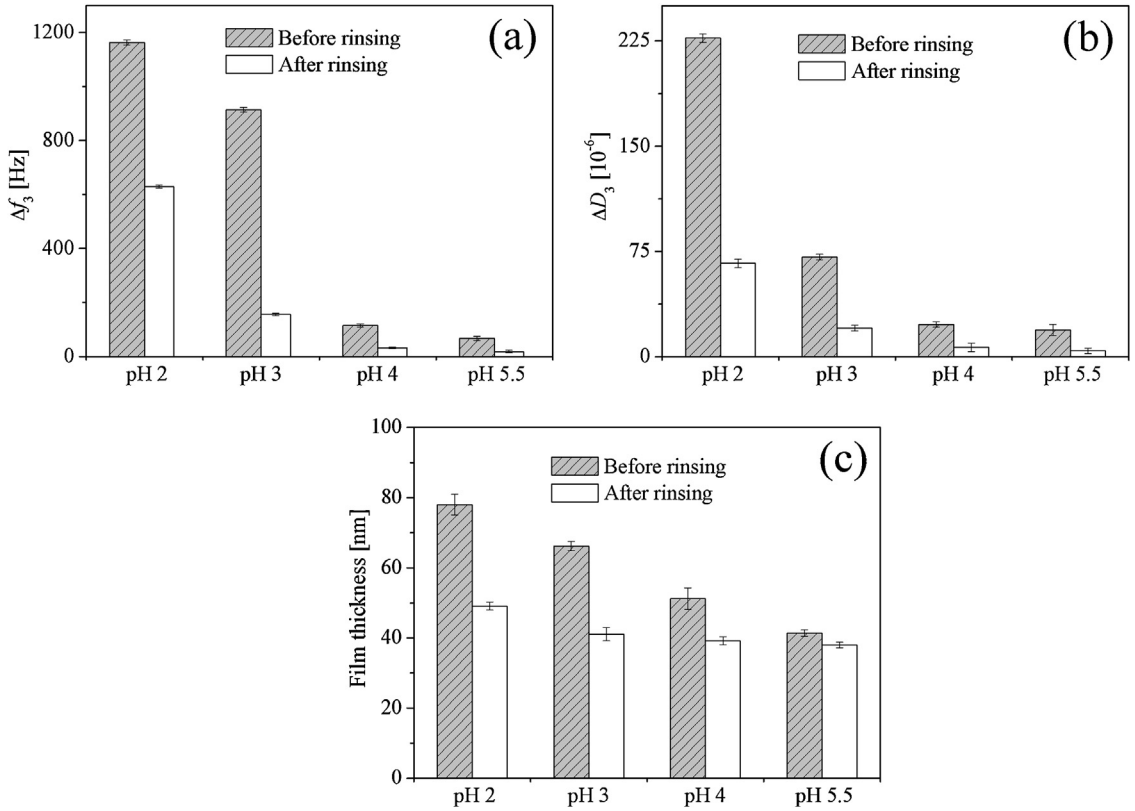

Fig. 6. Comparison of QCM-D frequency (a) and dissipation (b) change with film thickness (c) of three bilayers (from method II) obtained before and after rinsing with 5 M NaCl–50 mM HCl. *Note*: The pH values shown in the figure indicate the pH of the CMC solution (0.1%) during the coating.

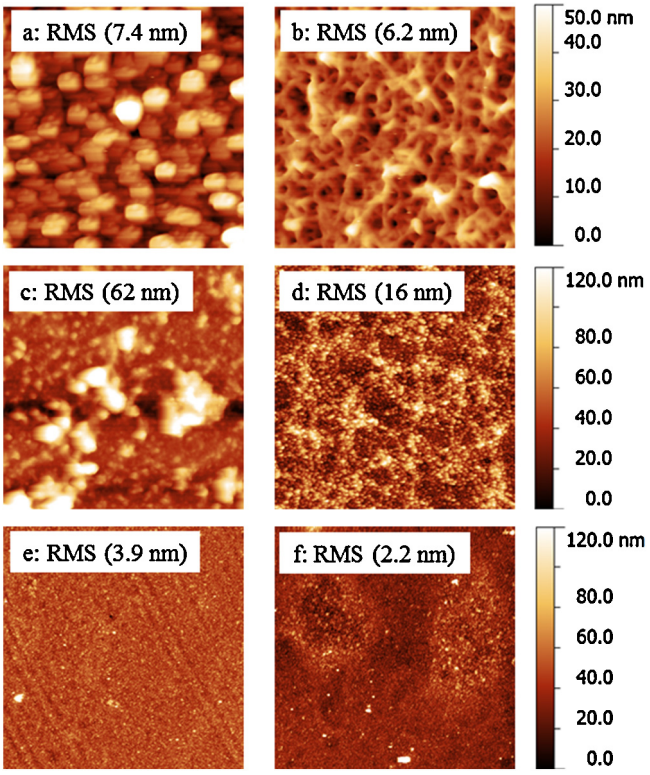

Fig. 7. Top row: AFM height images ($1 \times 1\ \mu m^2$) of three bilayers built up from CHI and CMC at pH 5.5 in 150 mM KCl on a DCA film pre-coated with CMC (a) and non-pre-coated (b). Middle and bottom row: AFM height images ($10 \times 10\ \mu m^2$) of three bilayers built-up from CHI at pH 5.5 in 150 mM KCl and CMC at different pH values ((c) pH 2; (d) pH 3; (e) pH 4; (f) pH 5.5) pre-coating with CMC at pH 2.

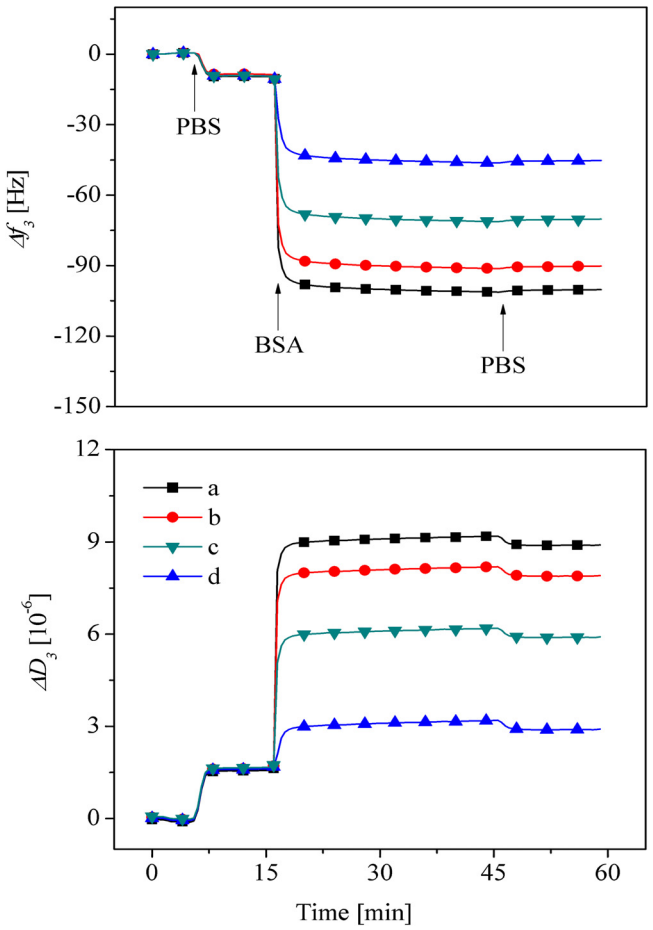

Fig. 8. QCM-D change in frequency (top) and dissipation (bottom) of BSA (10 mg ml^{-1}, dissolved in PBS buffer) adsorption at pH 7.4 on DCA films and on multilayers prepared from CHI and CMC at different pH values according to method II. (a) DCA film, (b) CMC at pH 5.5, (c) CMC at pH 3, (d) CMC at pH 2.

the pH of the CMC solution increases. These further evidences that larger amounts of polyelectrolyte are deposited at lower pH values which is in good correlation with the results obtained from QCM-D and film thickness measurements.

3.6. Protein adsorption

In order to demonstrate the potential applicability of the developed coatings as antifouling surfaces, the adsorption of BSA on multilayers fabricated according to method II was investigated. The BSA adsorption at pH 7 on DCA films and three bilayer coatings prepared from CHI and CMC at pH 2, 3, 5.5 is shown in Fig. 8. Before BSA application, the films were equilibrated with a PBS buffer until a constant frequency was established. As soon as the BSA solution was introduced, a strong decrease in frequency is noted which reached a plateau within 10 min. Upon rinsing with PBS buffer no significant increase in frequency is detected, confirming an irreversible protein adsorption. Maximum adsorption is noticed on DCA films. DCA is uncharged and has a partially hydrophobic character, as supported by IR and SCA data (see Fig. 1). Whereas BSA is negatively charged at pH 7, it contains hydrophobic residues, and can adsorb on both hydrophilic and hydrophobic surfaces (Raspor, 1991). Coatings obtained from CMC at pH 5.5 showed 10% less BSA adsorption ($f_3 = -90 \pm 2.1$ Hz) compared to DCA films ($f_3 = -100 \pm 1.9$ Hz). With decreasing pH of the CMC solution, a further reduction in the BSA adsorption can be observed. The carboxyl groups of the topmost CMC layer are negatively charged at pH 7. The interaction of BSA with the anionic CMC layer will therefore lead to electrostatic repulsion (Orelma, Filpponen, Johansson, Laine, & Rojas, 2011). This effect is assumed to be highly pronounced for the coatings obtained from CMC at pH 3 and 2 owing to the high charge density of carboxylic groups of the final CMC layer. Another explanation for the lower protein adsorption can be correlated with the presence of a hydration layer. As seen in Figs. 4–5, the final CMC coatings at pH 2 show a hydrophilic character (SCA(H_2O) = $4.3 \pm 0.5°$, Fig. 5b) and a dissipation change (Fig. 4, bottom) compared to coatings obtained at other pH values and to DCA films, indicating formation of a highly swollen structure with large amounts of incorporated water. Such a hydrated layer forms a high energetic barrier to prevent BSA adsorption. To facilitate protein adsorption water molecules surrounding the surface of the CMC layer and the BSA molecules have to be expelled (Chen, Li, Zhao, & Zheng, 2010). The stronger the hydrated layer is bound (*i.e.* higher dissipation change) the higher is the energy barrier, and thus the lower the protein adsorption. This explains why coatings fabricated from CMC at pH 2 are more resistance to BSA adsorption than less hydrophilic ones. Based on these results, we can conclude that the protein adsorption can be influenced by the chemical composition and hydrophilicity of the layers.

4. Conclusion

Simple LbL methods for creating antifouling coatings from the alternating deposition of hydrophilic polysaccharide multilayers of chitosan (CHI) and carboxymethyl cellulose (CMC) on partially deacetylated cellulose acetate (DCA) films were developed in this study. Deacetylation was necessary to increase the reactivity of cellulose acetate (CA) and irreversibly immobilize the multi-layers. Upon treatment of CA with potassium hydroxide, hydrophilicity is

increased and film thickness is reduced as confirmed by contact angle and Sarfus-thickness measurement. From method I, it was found that an initial anionic CMC pre-coating on DCA enhances the amount of deposited positively charged CHI and subsequently CMC owing to decreased solubility and charge, and thus leading to increased surface wettability and the layer thickness of the coatings. Whereas, from method II, it has been demonstrated that a low pH value (*i.e.* at a pH below the p*K* value) and decreased solubility of CMC solutions is favorable for the immobilization of higher amounts of CMC. The adsorbed mass and layer-thickness of multilayers increases as the pH of the CMC solution is decreased. The layers could be detached by high ionic strengths and low pH, showing their reliability as removable hydrophilic functional coatings for cellulose acetate. Further studies on the fouling properties of multilayers revealed that, compared to DCA films, BSA adsorption is reduced by 55% on coatings made from CMC at pH 2.

Acknowledgment

The research leading to these results has received funding from the European Union Seventh Framework Programme (FP7/2007-2013) under grant agreement no. 214653. The authors acknowledge the financial support from the Ministry of Education, Science and Sport of the Republic of Slovenia through the program no. P2 0118.

Appendix A. Supplementary data

Supplementary data associated with this article can be found, in the online version, at http://dx.doi.org/10.1016/j.carbpol.2014.04.068.

References

Ausserré, D., & Valignat, M.-P. (2006). Wide-field optical imaging of surface nanostructures. *Nano Letters*, *6*(7), 1384–1388.

Bauer, S., Arpa-Sancet, M. P., Finlay, J. A., Callow, M. E., Callow, J. A., & Rosenhahn, A. (2013). Adhesion of marine fouling organisms on hydrophilic and amphiphilic polysaccharides. *Langmuir*, *29*(12), 4039–4047.

Bulwan, M., Wójcik, K., Zapotoczny, S., & Nowakowska, M. (2012). Chitosan-based ultrathin films as antifouling, anticoagulant and antibacterial protective coatings. *Journal of Biomaterials Science, Polymer Edition*, *23*(15), 1963–1980.

Čakara, D., Fras, L., Bračič, M., & Kleinschek, K. S. (2009). Protonation behavior of cotton fabric with irreversibly adsorbed chitosan: A potentiometric titration study. *Carbohydrate Polymers*, *78*(1), 36–40.

Chen, S., Li, L., Zhao, C., & Zheng, J. (2010). Surface hydration: Principles and applications toward low-fouling/nonfouling biomaterials. *Polymer*, *51*(23), 5283–5293.

Dixon, M. C. (2008). Quartz crystal microbalance with dissipation monitoring: Enabling real-time characterization of biological materials and their interactions. *Journal of Biomolecular Techniques*, *19*(3), 151–158.

Findenig, G., Kargl, R., Stana-Kleinschek, K., & Ribitsch, V. (2013). Interaction and structure in polyelectrolyte/clay multilayers: A QCM-D study. *Langmuir*, *29*(27), 8544–8553.

Findenig, G., Leimgruber, S., Kargl, R., Spirk, S., Stana-Kleinschek, K., & Ribitsch, V. (2012). Creating water vapor barrier coatings from hydrophilic components. *ACS Applied Materials & Interfaces*, *4*(6), 3199–3206.

Fras, L., Laine, J., Stenius, P., Stana-Kleinschek, K., Ribitsch, V., & Doleček, V. (2004). Determination of dissociable groups in natural and regenerated cellulose fibers by different titration methods. *Journal of Applied Polymer Science*, *92*(5), 3186–3195.

Fujimoto, J., & Petri, D. F. S. (2000). Adsorption behavior of carboxymethylcellulose on amino-terminated surfaces. *Langmuir*, *17*(1), 56–60.

Glinel, K., Moussa, A., Jonas, A. M., & Laschewsky, A. (2002). Influence of polyelectrolyte charge density on the formation of multilayers of strong polyelectrolytes at low ionic strength. *Langmuir*, *18*(4), 1408–1412.

Hadj Lajimi, R., Ferjani, E., Roudesli, M. S., & Deratani, A. (2011). Effect of LbL surface modification on characteristics and performances of cellulose acetate nanofiltration membranes. *Desalination*, *266*(1–3), 78–86.

Han, B., Zhang, D., Shao, Z., Kong, L., & Lv, S. (2013). Preparation and characterization of cellulose acetate/carboxymethyl cellulose acetate blend ultrafiltration membranes. *Desalination*, *311*(0), 80–89.

Hayama, M., Yamamoto, K. i., Kohori, F., & Sakai, K. (2004). How polysulfone dialysis membranes containing polyvinylpyrrolidone achieve excellent biocompatibility? *Journal of Membrane Science*, *234*(1–2), 41–49.

Hoogendam, C. W., de Keizer, A., Cohen Stuart, M. A., Bijsterbosch, B. H., Smit, J. A. M., van Dijk, J. A. P. P., van der Horst, P. M., & Batelaan, J. G. (1998). Persistence length of carboxymethyl cellulose as evaluated from size exclusion chromatography and potentiometric titrations. *Macromolecules*, *31*(18), 6297–6309.

Höök, F., Rodahl, M., Brzezinski, P., & Kasemo, B. (1998). Energy dissipation kinetics for protein and antibody–antigen adsorption under shear oscillation on a quartz crystal microbalance. *Langmuir*, *14*(4), 729–734.

Iturri Ramos, J. J., Stahl, S., Richter, R. P., & Moya, S. E. (2010). Water content and buildup of poly(diallyldimethylammonium chloride)/poly(sodium 4-styrenesulfonate) and poly(allylamine hydrochloride)/poly(sodium 4-styrenesulfonate) polyelectrolyte multilayers studied by an in situ combination of a quartz crystal microbalance with dissipation monitoring and spectroscopic ellipsometry. *Macromolecules*, *43*(21), 9063–9070.

Jeyachandran, Y. L., Mielczarski, E., Rai, B., & Mielczarski, J. A. (2009). Quantitative and qualitative evaluation of adsorption/desorption of bovine serum albumin on hydrophilic and hydrophobic surfaces. *Langmuir*, *25*(19), 11614–11620.

Jones, K. L., & O'Melia, C. R. (2001). Ultrafiltration of protein and humic substances: Effect of solution chemistry on fouling and flux decline. *Journal of Membrane Science*, *193*(2), 163–173.

Kästner, U., Hoffmann, H., Dönges, R., & Hilbig, J. (1997). Structure and solution properties of sodium carboxymethyl cellulose. *Colloids and Surfaces A: Physicochemical and Engineering Aspects*, *123–124*(0), 307–328.

Kargl, R., Mohan, T., Bračič, M., Kulterer, M., Doliška, A., Stana-Kleinschek, K., & Ribitsch, V. (2012). Adsorption of carboxymethyl cellulose on polymer surfaces: Evidence of a specific interaction with cellulose. *Langmuir*, *28*(31), 11440–11447.

Kim, D.-Y., Nishiyama, Y., & Kuga, S. (2002). Surface acetylation of bacterial cellulose. *Cellulose*, *9*(3-4), 361–367.

Kontturi, E., Thüne, P. C., & Niemantsverdriet, J. W. (2003). Cellulose model surfacessimplified preparation by spin coating and characterization by X-ray photoelectron spectroscopy, infrared spectroscopy, and atomic force microscopy. *Langmuir*, *19*(14), 5735–5741.

Kontturi, K. S., Tammelin, T., Johansson, L.-S., & Stenius, P. (2008). Adsorption of cationic starch on cellulose studied by QCM-D. *Langmuir*, *24*(9), 4743–4749.

Koseoglu-Imer, D. Y., Dizge, N., & Koyuncu, I. (2012). Enzymatic activation of cellulose acetate membrane for reducing of protein fouling. *Colloids and Surfaces B: Biointerfaces*, *92*(0), 334–339.

Kutowy, O., & Sourirajan, S. (1975). Cellulose acetate ultrafiltration membranes. *Journal of Applied Polymer Science*, *19*(5), 1449–1460.

Laine, J., Lindstrom, T., Nordmark, G. G., & Risinger, G. (2002). Studies on topochemical modification of cellulosic fibres. Part 2. The effect of carboxymethyl cellulose attachment on fibre swelling and paper strength. *Nordic Pulp & Paper Research Journal*, *17*(1), 50–56.

Lee, J., Ryu, J., & Youn, H. (2012). Conductive paper through LbL multilayering with conductive polymer: Dominant factors to increase electrical conductivity. *Cellulose*, *19*(6), 2153–2164.

Liu, G., Zhao, J., Sun, Q., & Zhang, G. (2008). Role of chain interpenetration in layer-by-layer deposition of polyelectrolytes. *The Journal of Physical Chemistry B*, *112*(11), 3333–3338.

Liu, G., Zou, S., Fu, L., & Zhang, G. (2008). Roles of chain conformation and interpenetration in the growth of a polyelectrolyte multilayer. *The Journal of Physical Chemistry B*, *112*(14), 4167–4171.

Mohan, T., Kargl, R., Doliška, A., Vesel, A., Köstler, S., Ribitsch, V., & Stana-Kleinschek, K. (2011). Wettability and surface composition of partly and fully regenerated cellulose thin films from trimethylsilyl cellulose. *Journal of Colloid and Interface Science*, *358*(2), 604–610.

Mohan, T., Spirk, S., Kargl, R., Doliška, A., Ehmann, H. M. A., Köstler, S., Ribitsch, V., & Stana-Kleinschek, K. (2012). Watching cellulose grow—Kinetic investigations on cellulose thin film formation at the gas–solid interface using a quartz crystal microbalance with dissipation (QCM-D). *Colloids and Surfaces A: Physicochemical and Engineering Aspects*, *400*(0), 67–72.

Orelma, H., Filpponen, I., Johansson, L.-S., Laine, J., & Rojas, O. J. (2011). Modification of cellulose films by adsorption of CMC and chitosan for controlled attachment of biomolecules. *Biomacromolecules*, *12*(12), 4311–4318.

Radeva, T., Kamburova, K., & Petkanchin, I. (2006). Formation of polyelectrolyte multilayers from polysaccharides at low ionic strength. *Journal of Colloid and Interface Science*, *298*(1), 59–65.

Raspor, B. (1991). Adsorption of BSA from seawater at differently charged mercury surfaces. *Journal of Electroanalytical Chemistry and Interfacial Electrochemistry*, *316*(1–2), 223–234.

Rodahl, M., Höök, F., Krozer, A., Brzezinski, P., & Kasemo, B. (1995). Quartz crystal microbalance setup for frequency and Q-factor measurements in gaseous and liquid environments. *Review of Scientific Instruments*, *66*(7), 3924–3930.

Schlenoff, J. B., Rmaile, A. H., & Bucur, C. B. (2008). Hydration contributions to association in polyelectrolyte multilayers and complexes: Visualizing hydrophobicity. *Journal of the American Chemical Society*, *130*(41), 13589–13597.

Schoeler, B., Kumaraswamy, G., & Caruso, F. (2001). Investigation of the influence of polyelectrolyte charge density on the growth of multilayer thin films prepared by the layer-by-layer technique. *Macromolecules*, *35*(3), 889–897.

Schoeler, B., Poptoshev, E., & Caruso, F. (2003). Growth of multilayer films of fixed and variable charge density polyelectrolytes: Effect of mutual charge and secondary interactions. *Macromolecules*, *36*(14), 5258–5264.

Schönhoff, M., Ball, V., Bausch, A. R., Dejugnat, C., Delorme, N., Glinel, K., Klitzing, R., & Steitz, R. v. (2007). Hydration and internal properties of polyelectrolyte multilayers. *Colloids and Surfaces A: Physicochemical and Engineering Aspects*, *303*, 14–29.

Shiratori, S. S., & Rubner, M. F. (2000). pH-dependent thickness behavior of sequentially adsorbed layers of weak polyelectrolytes. *Macromolecules*, *33*(11), 4213–4219.

Yuan, W., Dong, H., Li, C. M., Cui, X., Yu, L., Lu, Z., & Zhou, Q. (2007). pH-controlled construction of chitosan/alginate multilayer film: Characterization and application for antibody immobilization. *Langmuir*, *23*(26), 13046–13052.

Zhang, J., Chen, X. G., Li, Y. Y., & Liu, C. S. (2007). Self-assembled nanoparticles based on hydrophobically modified chitosan as carriers for doxorubicin. *Nanomedicine: Nanotechnology, Biology and Medicine*, *3*(4), 258–265.

Zhang, S., Liu, W., Liang, J., Li, X., Liang, W., He, S., Zhu, C., & Mao, L. (2013). Buildup mechanism of carboxymethyl cellulose and chitosan self-assembled films. *Cellulose*, *20*(3), 1135–1143.